

## Dynamic Performance of Line Commutated Converter-Based Multiterminal HVDC Systems

**Abstract.** In this article, the modelling and simulation results related to the dynamic performance of a multiterminal HVDC system, based on Line Commutated Converters (LCC), is presented. The four-converter HVDC system simulated operates at 500 kV. In order to evaluate its behaviour in a more realistic way, the multiterminal HVDC system was embedded into an equivalent ac network that resembles an existing high voltage system. A model to represent the ac generator dynamics (speed regulator and voltage controller), which interacts with the DC system, is also presented in the paper. The converter blocking condition, which is another HVDC operative requirement, was also simulated. From the dynamic response of the converters and ac sources obtained, it can be stated that the LCC-based multiterminal HVDC system can be a good alternative to be considered while analysing issues like planning, expansion and transmission of bulk power.

**Streszczenie.** W artykule zaprezentowano modelowanie i symulację właściwości dynamicznych systemu HVDC bazującego na układzie Line Commutated Converter LCC. W celu oceny właściwości w bardziej realistycznych warunkach system HVDC został wbudowany w odpowiednią sieć AC co przypomina istniejące systemy wysokiego napięcia. Na podstawie badań stwierdzono że wieloterminowy system HVDC może być dobrą alternatywą dla istniejących systemów. **Właściwości dynamiczne wieloterminowego systemu HVDC wykorzystującego układy LCC**

**Keywords:** Dynamic Analysis, Fault conditions, HVDC, Line Commutated Converter (LCC), Multiterminal system.

**Słowa kluczowe:** właściwości dynamiczne, system HVDC, konwerter LCC

### Introduction

Recent technology developments in the power electronics industry enabled the installation of new LCC (Line Commutated Converter) and VSC (Voltage Source Converter) based HVDC systems worldwide. By the 1970s the point-to-point and back-to-back LCC technology (using solid state devices) had already reached a high level of maturity. Today, the LCC-based HVDC technology appears as one of the main alternatives to transmit bulk power over long distances.

As an example, it is foreseen that in 2015, the longest LCC-based HVDC system (delivering approximately 2x3150 MW at  $\pm 600$  kV, over 2500 km) will be in operation in Brazil. This DC system connects the northern part of the country, which has a high hydroelectric potential, to the southeast region where the main load centres are located.

As early as 1965 [1], the basic principles of multiterminal systems regarding HVDC lines were already established. Presumably due to technological issues (like the boom of the ac systems initiated in the 1960s) the LCC-based multiterminal HVDC technology did not recently witness the installation of new practical systems. So far, only two real multiterminal DC systems are in operation. The first one is the Hydro Québec – New England system, and the second is the Sardinia-Corsica-Italy system. It is expected that in 2014-15, a  $\pm 800$  kV, 6.000 MW LCC-based multiterminal HVDC system will start to operate in the North-East of India.

The fundamental concepts to control multiterminal DC systems, their parallel operation, as well as the challenges encountered with this technology can be found in [2]-[8]. Such references emphasise the coordination of the current order principle (balancing principle) so that each converter handles properly the allocated amount of power. Particularly in [7], the practical implementation of parallel multiterminal DC systems and the requirements for current order coordination are discussed. A detailed description of some of the most common two-terminal and multiterminal systems currently in operation is presented in [9]. In depth analysis on the DC filters and interference of multiterminal DC systems upon neighbouring equipment can be found in [10]. Although the use of its counterpart VSC-based HVDC technology appears as the trend for the establishment of future DC systems, it is still encountering some limitations which may delay its application for the transmission of bulk

power. Thus, it was deemed useful developing a study on the LCC-based HVDC technology on account of the following reasons:

- The VSC-based HVDC technology is still limited by the capacity of the available solid-state devices with turn-off capability. Some manufacturers, though, are currently announcing that they can deliver VSC converters with up to 1000 MW of capacity.
- At some time of their operation, existing LCC-based HVDC systems may be in need to be interconnected, thus, forming a specific DC network.

Unlike the aims of the references previously described, the objective of this article is to present the main aspects considered whilst modelling a multiterminal DC system and present the steady state and dynamic response of both the ac system (regarding the generator dynamics) and the DC system toward faults occurring at some points within the considered network. A model of the speed regulator and the voltage controller to represent the ac generator dynamics, which interact with the DC system, are also presented in the paper. The main LCC-based multiterminal HVDC configuration is the parallel connection of the converters, and it was adopted in this study (Fig. 1).

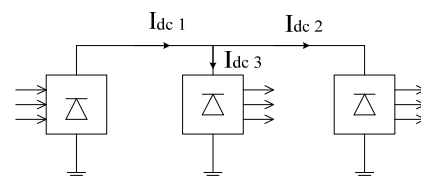


Fig.1. Parallel multiterminal HVDC configuration.

In the parallel configuration, all converters operate at the same rated DC voltage thus; the power control is primarily done through the DC current of the converters. Further information on these system configurations can be found in [1] and [13]. The PSCAD/EMTDC program, broadly used to simulate power systems, was used in this study.

One of the major disadvantages of a point-to-point HVDC system is the difficulty to tap or inject power at any point on the transmission line. This problem can be overcome through a multiterminal HVDC system in which power can be derived or injected at any point of the DC

system provided the existence of its respective converter. A multiterminal DC system could also be a solution in cases where various ac systems arriving to a collector substation have to necessarily be transformed into DC to subsequently transmit such bulk power over long distances. It is the case of the above mentioned Brazilian (Madeira) system whose dispersed generation and ac transmission join in one collector ac/dc substation for its subsequent transmission.

### Description of the Multiterminal HVDC System Used

In order to analyse a more realistic case, a four-terminal HVDC system, emulating the performance of what would be the two-rectifier and two-inverter DC system linking areas A1, A2 and A3 (see Fig. 2), was adopted.

The multiterminal DC system studied here was implemented regarding the HVDC benchmark proposed by [11]. The main parameters and characteristics of the multiterminal system to be considered are:

- The main DC line transmits 2000 MW at 500 kV. Thus, the rated power of each rectifier/inverter is 1000 MW.
- The DC line length common to the two rectifiers and two inverters is 1300 km (4x1510 MCM conductor with a resistance of 10 Ω/pole). The distance between Inverters 2 and 3 is approximately 300 km (4x954 MCM with a resistance of 5 Ω/pole). The reason for referring the Inverters as 2 and 3 (and not as 1 and 2) is because Rectifiers 1 and 2 can actually be seen as an equivalent rectifier. This is because the distance between them is very small; thus, it can be neglected. So, one can see three main converters (i.e. converters 1, 2 and 3).
- Only for ease of analysis the multiterminal DC system is represented as an equivalent monopole system without loss of generality. For the purposes of this article, the main concern is to show the dynamic response of the converters and the synchronous machines, hence the use of the referred configuration.

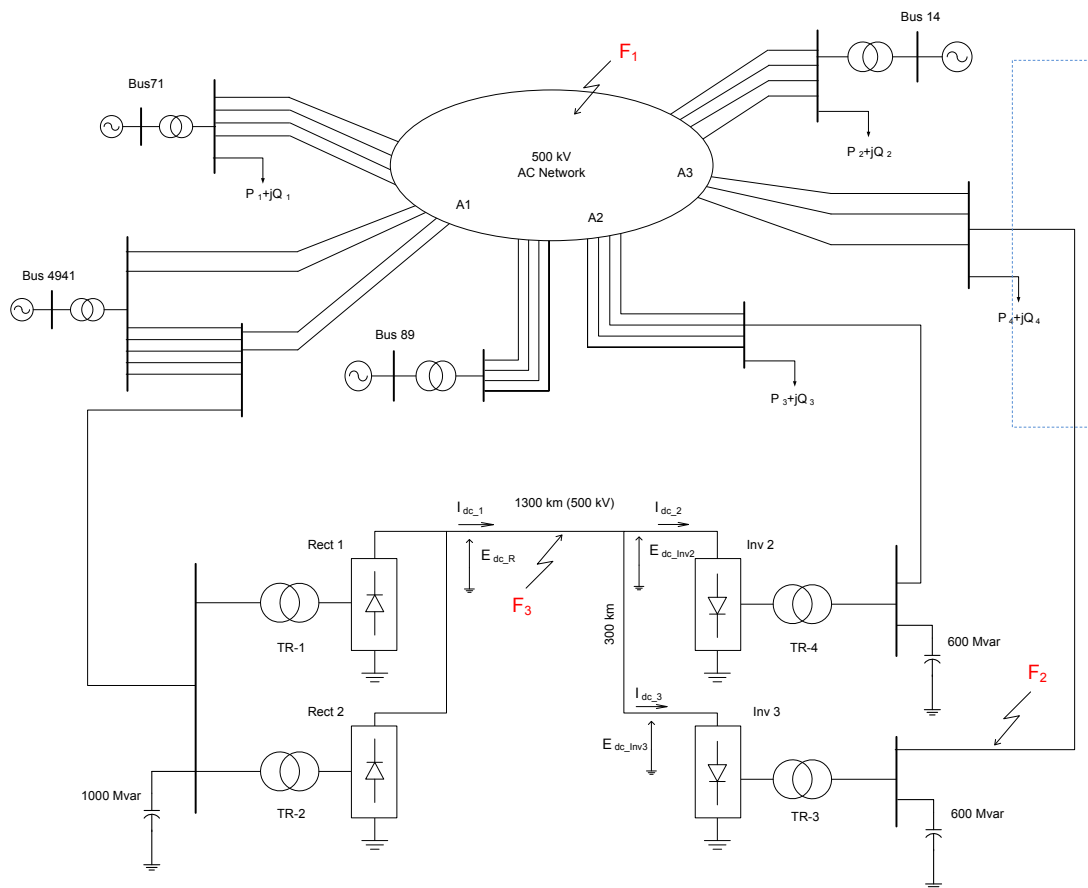


Fig.2. Multiterminal HVDC system inserted into the 500 kV ac grid.

The operation principle of the elementary 12-pulse thyristor bridge and its converter transformer is well known. Likewise, a description of the extinction ( $\gamma$ ), firing ( $\alpha$ ) and overlap angle ( $\mu$ ) need not be done, as they are similarly used as in point-to-point HVDC systems [14]. However, it is advised to bear in mind that  $\gamma = (180 - \alpha - \mu)$ .

The 12-pulse converter (specifically Rectifier 1) is shown in Fig. 3. Each 6-pulse sub-converter is connected to the ac grid through Y- $\Delta$  and YY transformers with tap changers. Note also the presence of the smoothing reactors ( $L_d$ ) and the DC parallel filter. As for the inverters (Inv 2 and Inv 3, also shown in Fig. 2), rather than directly dealing with the

firing angle ( $\alpha$ ), they will act upon the extinction angle ( $\gamma$ ). The minimum value of  $\alpha$  was set to 5°, while the minimum value of  $\gamma$  to 15°. The latter was adopted to ensure that there is enough time given for the commutation between valves

### Control System

The control diagram of the  $\alpha$  angle ( $\alpha_{OR}$  output) is shown in Fig. 4. Notice, among other features, the presence of the VDCOL (Voltage Dependent Current Order Limit) function and the calculation of the  $\beta$  angle ( $\alpha \leq 180^\circ - \beta$ ). Recall that the main objective of the VDCOL function is to improve both

the voltage and power stability during and after the occurrence of faults in the system. This control is responsible for reducing the current order according to the value of the DC voltage, which occurs whenever the ac voltage falls due to, for example, faults in the ac grid. Further details regarding this control function can be found in [12].

The input variables to control the  $\alpha$  angle (Fig. 4) are the converter output DC voltage ( $V_{dc\_R}$ ) and current ( $I_{dc\_R}$ ). The VDCOL function is compared with the reference current ( $I_o$ ). The minimum value of these variables is the current order ( $C_{ORD}$ ) which when compared to CMRS (i.e.  $I_{dc\_R}$  compensated with a gain function) gives the current error ( $C_{ERR}$ ). After passing through a PI (Proportional-Integral) controller, the  $C_{ERR}$  becomes the beta angle at the rectifier ( $\beta_R$ ) from which alpha is obtained ( $\alpha_{OR}=180-\beta$ ).

In a two-terminal HVDC system only one converter will control the current and the other one will control the voltage. As for the multiterminal system on a parallel scheme, only one converter controls the voltage and the rest of the converters will primarily control the current. Thus, it becomes necessary to use an enhanced master control to calculate and coordinate the reference current in each converter including also measuring and communication time delays.

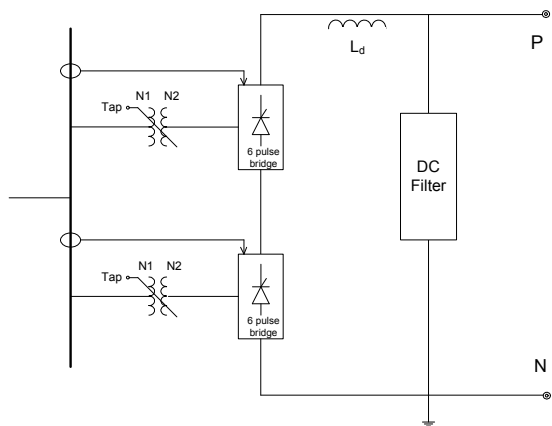


Fig.3. General model of the converters (Rectifier 1) used in the PSCAD/EMTDC program.

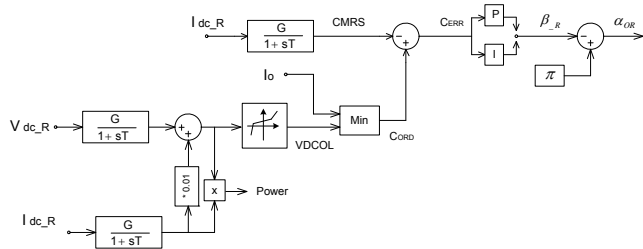


Fig.4. Alpha angle control of the rectifiers.

### Static Characteristic of the Multiterminal HVDC System

Although the article is mainly focussed on the dynamic behaviour of a multiterminal HVDC system, it is deemed worthy to present the basis of the start-up and steady-state operation so as to provide the reader an understanding of its coordination among the converters. Furthermore, the static characteristic of the multiterminal HVDC system is based on the general philosophy of a two-terminal HVDC line. The main difference is that in the former case the sum of the current orders ( $I_{OR}$ ) of all inverters and all rectifiers should be equal to zero. For the four-converter multiterminal HVDC system, this condition will be (1):

$$(1) \quad (I_{OR\_R1} + I_{OR\_R2}) = (I_{OR\_I2} + I_{OR\_I3})$$

In the case of the master control used (Fig. 5), it can be seen that  $I_{o\_R} = (I_{o2}+I_{o3})$ , in turn, the current in each rectifier (i.e. the percentage of current contribution to the DC link) is controlled through the  $K_c$  slider. In the converter that controls the voltage, the margin current ( $\Delta I_d$  in Fig. 6) should be added to its control system. Typically, the value of  $\Delta I_d$  is about 0.1 pu of  $I_{dc}$  [14].

Only for ease of the static characteristic representation, it will be assumed that Rectifier 1 and Rectifier 2 (Fig. 2) operate as an equivalent rectifier. Thus, for this simplified three-terminal system the static characteristic will be that shown in Fig. 6. On this regard, the following comments apply:

- The operating DC voltage is determined by Conv-2 (minimum voltage) which is operating under the constant extinction angle ( $\gamma$ ) control.
- For the considered condition, each converter operates at its Operating Point (OP) depicted in Fig. 6.
- Conv-3 is operating under the constant DC current control mode.
- The available current for Conv-2 results from the difference between  $I_{OR\_1} - I_{OR\_3}$ . The condition  $I_{OR\_1} > I_{OR\_3}$  applies here.

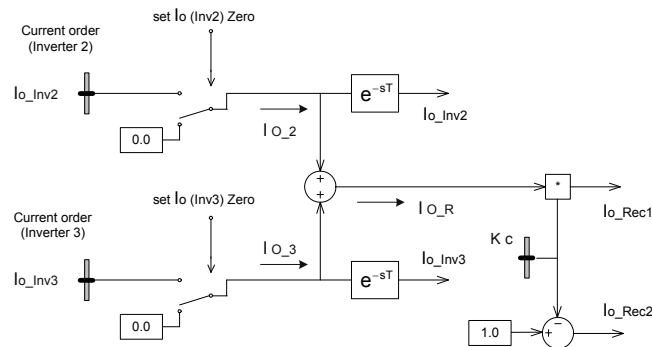


Fig.5. Simplified master control diagram of the three terminal HVDC system.

If for any reason, the voltage of Conv-3 becomes lower than the voltage of Conv-2, the current control will move to Conv-2; thus, Conv-3 will be the one determining the new DC voltage. Furthermore, this converter will now operate at constant extinction angle ( $\gamma$ ) control.

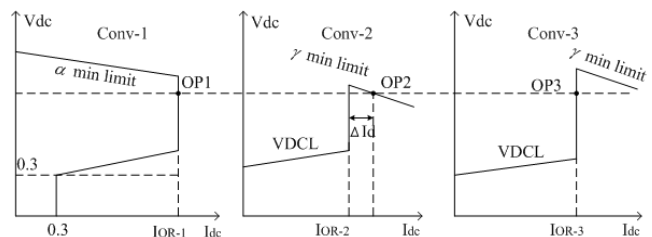


Fig.6. Static characteristic of the three-converter DC system.

It should be noted that the above ideal static characteristics address only the multiterminal behaviour at steady-state. Its behaviour at conditions other than such a state can be somewhat different. Normally, the communication system among terminals is an important requirement for a good control and operative coordination. As it can be observed in Fig. 4 the control method of the alpha angle ( $\alpha_{OR}$ ) driving the rectifiers and the master control presented in Fig. 5 are relatively simple. The master control, in particular, is based on balancing the total current

order entering Inverters 2 and 3. This makes the control system shown practical for other applications.

One of the problems linked to the operation of LCC-based converters (specifically the inverters) is the commutation failure. Briefly, the commutation failure occurs when the current from the turning off thyristor fails to transfer to the turning on thyristor. In other words, due to certain causes an inverter valve goes into short-circuit [15]. Studies have shown that among such causes resulting in commutation failure are: faults and voltage sags at the ac side of the inverter, temporary increase of the DC current, reduction of the extinction angle ( $\gamma$ ), thyristor triggering pulse errors, etc.

### Simulation Results

The first set of results presented in the article was obtained considering the four generators as ideal sources. This is done to initially test the behaviour of the multiterminal DC system implemented. The initialisation period shown at the beginning of each plot could have been omitted using, for example, the snapshot option available in the program used. However, it was left there so as to put in evidence how each variable reaches the steady-state operation. Indeed, such initialisation periods can be improved or made shorter. The second set of results considers the dynamic model of the generators (i.e. they will no longer be treated as ideal sources but it will consider the dynamics of each machine).

The active power transmitted by the DC link ( $P_{dc_1}$ ) and received by inverters 2 and 3 ( $P_{dc_2}$  and  $P_{dc_3}$ ) is shown in Fig. 7. The behaviour of the DC voltage at rectifier 1 and the inverters is shown in Fig. 8. It can be observed that after the initialisation process ( $0 < t < 0.5$  s) all the measured variables start operating around the target values until they eventually become stable and constant.

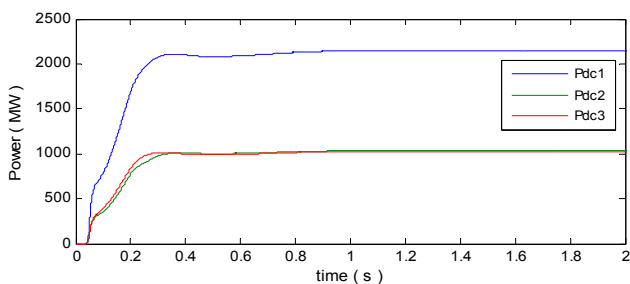


Fig.7. Power transmitted in the DC link and received by the inverters.

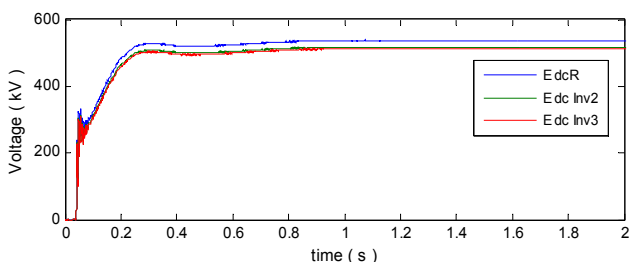


Fig.8. DC voltage near the rectifier and close to inverters 2 and 3.

The values of  $\alpha$  (Rectifier 1) and  $\gamma$  (inverters) are presented in Fig.s 9(a) and 9(b). Note that the firing angle ( $\alpha \approx 19.06^\circ$ ) is operating close to typical values encountered in HVDC systems. The value of  $\alpha$  in the second rectifier (Rectifier 2) was practically equal as that of Rectifier 1. Based on the values of the extinction angle ( $\gamma$ ) at steady-state, it can be stated that Inverter 2 ( $\gamma \approx 17.54^\circ$ ) is controlling the voltage and Inverter 3 ( $\gamma \approx 24.42^\circ$ ) is controlling the current.

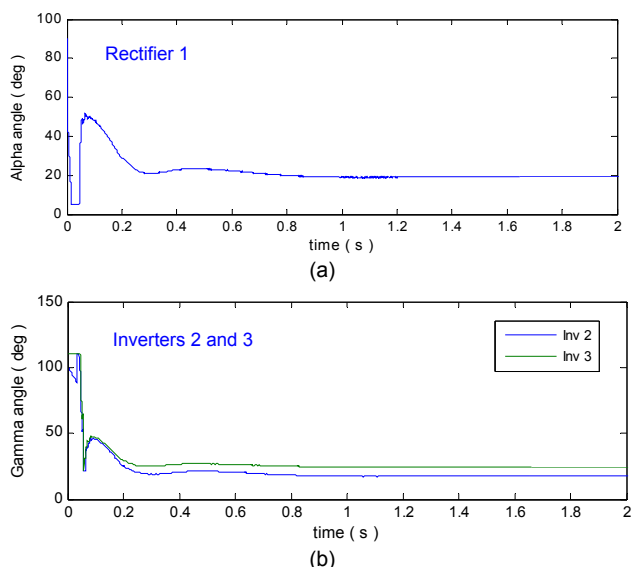


Fig. 9. Value of: (a) Alpha at the rectifiers, (b) Gamma at the inverters.

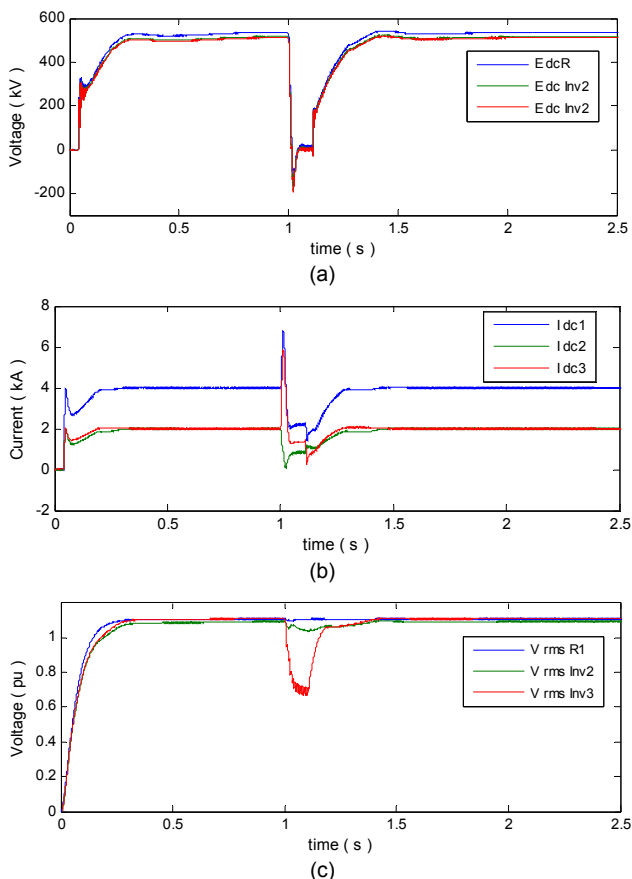


Fig.10. Behavior of the rectifiers and inverters 2 and 3 during the fault: (a) DC voltage, (b) DC current, (c) per unit rms voltage (AC side).

### Application of Faults in the System

In order to evaluate the performance of the multiterminal system towards dynamic conditions, some faults in the ac side of the converters were applied (see the location of  $F_1$  and  $F_2$  in Fig. 2). Still, only the results corresponding to fault  $F_2$  (close to transformer TR-3) will be shown. The  $F_1$  fault (within the 500 kV ac network) did not affect significantly the HVDC system. It was also observed that faults occurring at the ac side of the rectifiers did not cause a significant stress upon the converters. Conversely, ac faults close to Inverter

2 did cause a relatively higher adverse effect upon both ac and DC systems. The ideal switch emulating the fault (phase-to-ground fault) was set to close at  $t = 1.0$  s and open after 100 ms. Faults in other parts of the system were also simulated, but the results presented here were the most important for the system as a whole.

### a) Phase-to-ground fault close to inverter 3 ( $F_2$ )

The DC voltage and current measured in the converters are shown in Figs 10(a) and (b). The major effect occurs upon Inverter 3 (Fig. 10c) which presents a higher voltage drop ( $V_{rms\_inv3}$ ). Recall that the controls in the rectifier normally control the transmitted DC current and the controls in the inverter usually regulate the DC voltage.

In order to protect and block the DC fault current during the fault period, not shown here though, the  $\alpha$  angle in both rectifiers will rise up to about  $90^\circ$ , returning to their pre-fault value once the fault is cleared.

At any instant, the master control will balance the DC current among all converters. In Fig. 10(b), for example, the current in all converters, prior to the application of the fault, is balanced. Once the fault is cleared the current order within the master control restores the target values to those present during the pre-fault state.

The current overshoot observed in Fig. 10(b), reaching approximately 7 kA, is due to the commutation failure caused by the sudden increase of the DC current and the drop of the ac voltage in the inverter side (Fig. 10c). The next action, i.e. limiting the DC current to its minimum target value, is taken by the VDCOL control as a means to protect the converter and its associated components.

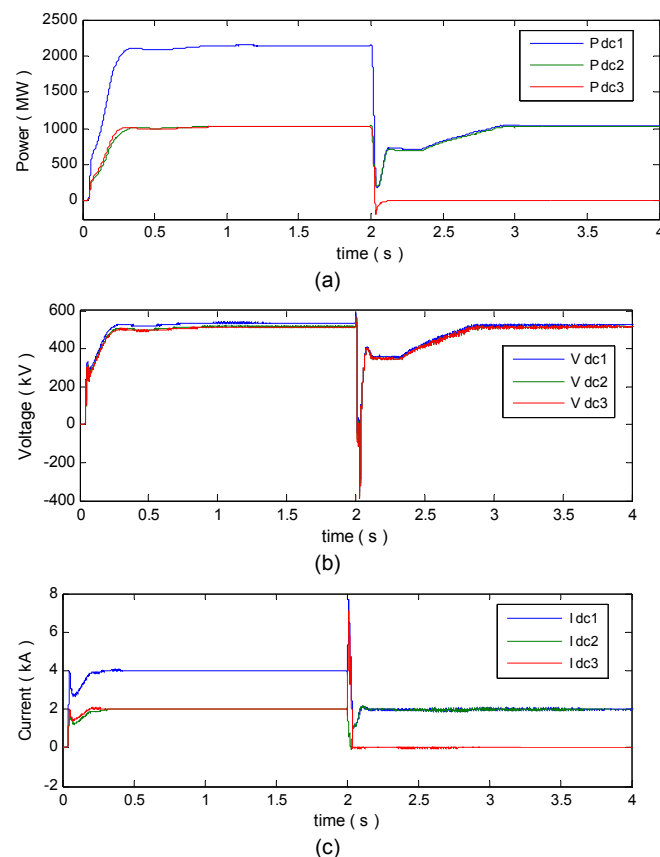


Fig. 11. (a) Power in the DC link, (b) DC link voltages, (c) DC currents.

### b) Faults in the DC Line ( $F_3$ )

The response of the multiterminal DC system towards a fault occurring in the 1300 km DC line (pole-to-ground fault)

was also simulated. The mid line fault was represented through an ideal switch placed between the line (positive pole) and the ground ( $R_{fault}=0.001\Omega$ ). The duration of the fault was equal to 200 ms. The VDCOL detects the DC voltage drop and quickly reduces the current order in the system, which favours the short-circuit extinction without the need to open the affected line. Due to this fast action the event turned to be less stressing for the system and the converters resumed their normal operation as soon as the fault was cleared. For this reason the results corresponding to this type of fault are not included here.

### c) Converter Blocking

There may be cases where blocking the converters (i.e. removing the control pulses from the thyristors) become inevitable, especially during the occurrence of internal faults, errors during the power control, excessive ac voltage drop, etc.

In order to show the response of the multiterminal HVDC system towards this condition, Inverter 3 was blocked at  $t = 2.0$  s, as shown in Fig. 11.

From  $t=0.0 \rightarrow 2.0$ s, each inverter of the multiterminal system delivers 50% of the transmitted power (Fig. 11a). After this time period (i.e. with Inverter 3 already blocked) only Inverter 2 remains transmitting its rated power through the DC link ( $t = 2.0 \rightarrow 4.0$ s). In this case, the master control has to adjust the current order so that only 50% of the normal power is sent by the rectifiers. The other 50% power blocked in the DC link ( $\approx 1000$  MW) will flow through other routes inside the AC system.

Reversing the blocking condition (i.e. blocking Inverter 2 and letting Inverter 3 operating) requires redefining the converters' static characteristic to see which converter is going to control the voltage. Also, the master control has to rearrange the current order in the remaining converters.

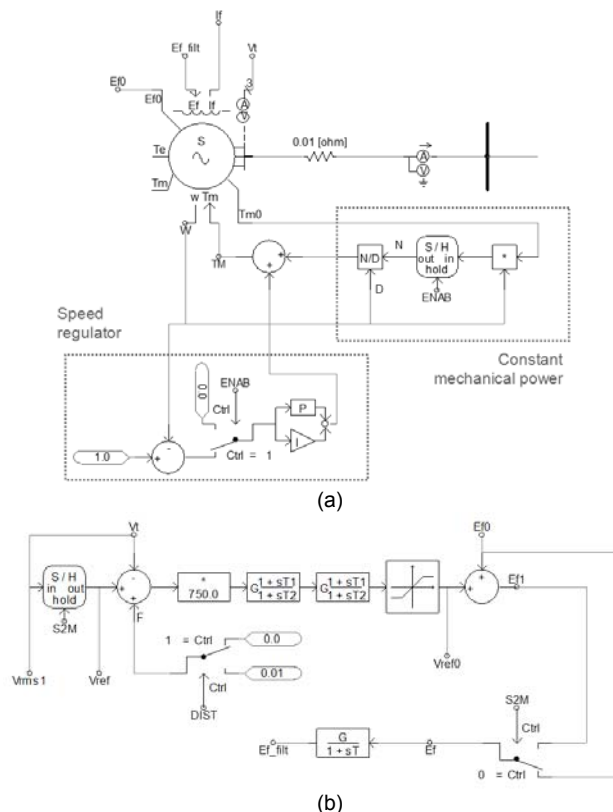


Fig.12. (a) Machine model used at buses 14, 71, 89 and 4941 to observe the system dynamic response, (b) voltage regulator.

### Response of the Multiterminal HVDC System Regarding the Machine Dynamics

In this section, the generators initially represented as ideal sources were replaced by salient pole hydro-generators including their dynamic models. This implied the specification of the  $d$ - $q$  synchronous, transient and sub-transient reactances and time constants, inertia constants, as well as the use of a speed regulator and a constant mechanical power loop (Fig. 12a). The voltage regulator used in all the machines is shown in Fig. 12(b). In this study, the fault is applied at  $t = 4.5$  s and removed after 100 ms. The integration time step used to simulate the system dynamic stability ( $\Delta t = 100 \mu s$ ) is regarded as sufficient to get the expected results. Smaller time steps will be required as the complexity of the system increases (e.g. dedicated representation of the line model, etc).

The results of the converters, under this new system condition, are not included in the article. This is because, except for some minor power oscillations which were quickly damped, the multiconverter system presented nearly the same response with both ideal sources and with the synchronous machines modelled as quasi real machines. However, it was found appropriate to include the results of the power, speed, voltage, angle and torque oscillations of the equivalent ac machines and their subsequent stabilization.

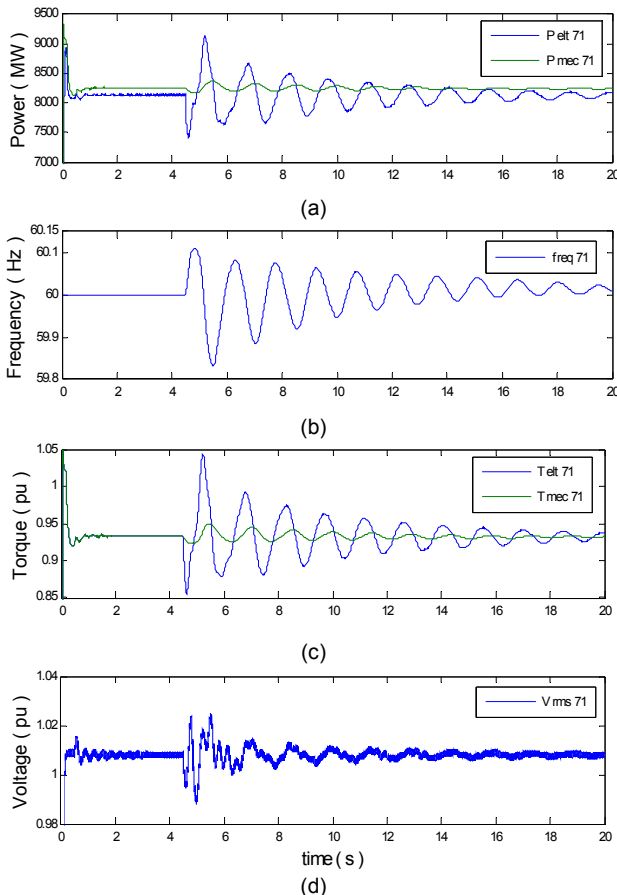


Fig.13. Response of the machine connected to Bus 71 towards the fault  $F_2$ : (a) electrical & mechanical power, (b) frequency, (c) electrical & mechanical torque, (d) rms terminal voltage.

### Phase-to-ground fault ( $F_2$ ) on the AC side of Inverter 3

As for the phase-to-ground fault ( $F_2$ ) occurring in the AC side of Inverter 3, the initial characteristic oscillation and subsequent damping of the variables requested is shown in Fig. 13.

The names appearing in the upper right side of Fig. 13(a) refer to the electric and mechanical powers ( $P_{elt\_71}$  and  $P_{mect\_71}$ ) of the equivalent generator connected to bus 71. The machine frequency ( $F_{req\_71}$ ) and the electric and mechanical torque ( $T_{elt\_71}$  and  $T_{mect\_71}$ ), are shown in Figs 13(b) and 13(c), respectively. The rms terminal voltage ( $V_{71\_rms}$ ) is shown in Fig. 13(d).

Due to the proximity between Inverters 1 and 2, it was also observed that the voltage and output power of these inverters were the most affected. Indeed, should Inverter 2 be further from Inverter 3 (regarding the occurrence of fault  $F_2$ ), the effect of the fault upon Inverter 2 would be much smaller. This type of fault and location may cause commutation failure in the converter valves.

The behaviour of the DC link power and voltage during the fault (at the sending end) is shown in Figs 14(a) and (b), respectively. Last, the recuperation of  $\alpha$  (Rectifier 1) and  $\gamma$  (Inverter 3) during and after the fault is cleared is shown in Figs 15(a) and (b), respectively. All machines returned to their pre-fault operative condition once the fault was removed, which means that both the speed regulator and the voltage controller model implemented in each machine (generator) are robust toward the disturbances imposed in the system.

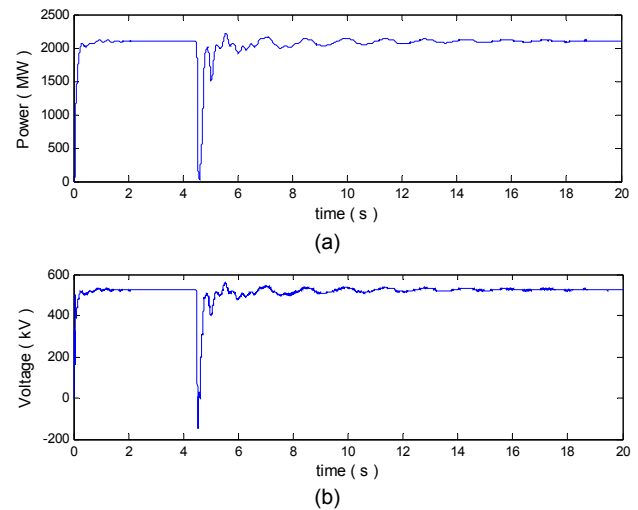


Fig.14. (a) DC power and, (b) DC voltage measured at the sending end of the DC line (phase-to-ground fault,  $F_2$ ).

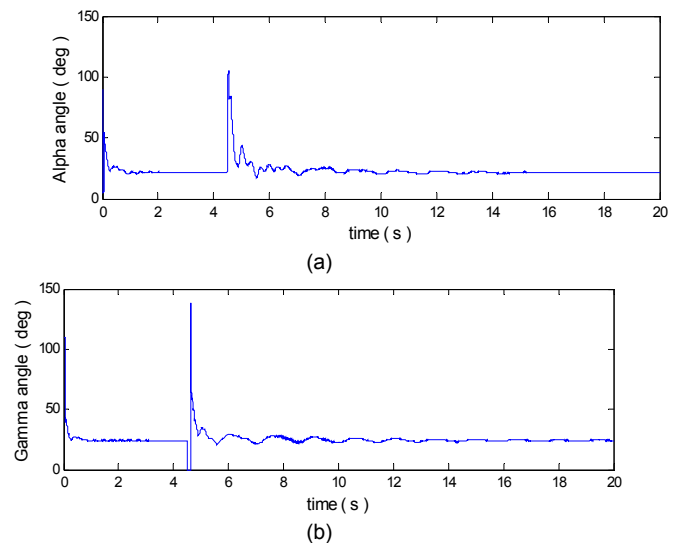


Fig.15. (a) Alpha angle of Rectifier 1 during the fault ( $F_4$ ), (b) Gamma angle of Inverter 3.

## Conclusions

Through the simulation results presented herein, it was shown that an LCC-based multiterminal HVDC system can well be a feasible alternative for the interconnection of DC systems carrying bulk power. The dynamic response of the four-converter HVDC system inserted into the 500 kV ac network, regarding some imposed disturbances, showed a satisfactory performance. A similar response was observed regarding its steady-state performance. These results demonstrate that LCC-based HVDC systems that currently operate under a point-to-point scheme could have a satisfactory operation when connected to form a DC multiterminal network, provided an adequate control system and current coordination among its converters. On this regard, the master control used in the model would adequately respond during and after the presence of transient events (such as faults) as well as during converter blocking actions.

Unlike point-to-point HVDC systems, defining which converter will operate as constant extinction angle or constant DC current mode in multiterminal DC systems is highly significant. In this article, Converter 2 operates under the constant extinction angle ( $\gamma$ ) control, whereas Converter 3 operates under the constant DC current control mode. The control method of the alpha angle driving the rectifiers and the master control presented are relatively simple and practical for future applications.

## Appendix

Main constants used for the alpha angle control shown in Fig. 4:

$$G = 0.5; T = 0.0012; P = 1.099; I = 0.011$$

Main constants used in the machine(s) model (i.e. generator shown in Fig. 12):

$$G_1 = 1.0; T_1 = 1.96; T_2 = 18.6; P = 5.0; I = 40; G = 1.0; T = 0.005$$

All data used in this article can be willingly sent upon request.

## Acknowledgment

The authors gratefully acknowledge ANEEL (Brazilian Energy Regulatory Agency) for the support provided. Special thanks go to Paulo Fischer (Ph.D. Eng.) for his valuable help provided while working with the multiconverter DC system.

## REFERENCES

- [1] Reeve J.; Multiterminal HVDC Power Systems, *IEEE Trans. Power Apparatus and Systems*, Vol. PAS-99, no. 2, pp. 729-737, Mar/Apr 1980.
- [2] Lamm U.; Uhlmann E. and Danfors P.; Some Aspects of Tapping HVdc Transmission Systems, *Direct Current*, Vol. 8, No. 5, pp. 124-129, May 1963.

- [3] Reeve J. and Arrillaga J.; Series Connection of Converter Stations in an HVDC Transmission System, *Direct Current*, Vol. 10, No. 2, pp. 72-78, May 1965.
- [4] Martensson H. and Adielson T.; Simulator Studies of Multiterminal HVDC Systems, Conf. on *HVDC Transmission*, IEEE Conf. Publ. No. 22, pp. 134-145, Manchester 1966.
- [5] Ekstrom A.; Juhlin L.-E.; Liss G.; Parallel Connection of Converters for HVDC Transmissions, *IEEE Trans. Power Apparatus and Systems*, Vol. PAS-97, No. 3, pp. 714-724, May/June 1978.
- [6] Kanngiesser K.W.; Bowles J.P.; Ekstrom A.; Reeve J.; Rumpf E.; HVDC Multiterminal Systems, *Cigré paper SC 14-08*, 1974.
- [7] Nozari F.; Grund C.E.; Haut R.L.; Current order Coordination in Multiterminal DC Systems, *IEEE Trans. Power Apparatus and Systems*, Vol. PAS-100, No. 11, pp. 4628-4635, Nov 1981.
- [8] Hauth R.L.; Nozari F.; Breuer G.D.; Melvold D.J.; Multiterminal HVDC Control Techniques for Future Integrated AC-DC Networks, *Cigré paper 14-01*, 1982.
- [9] Long W.F.; Reeve J.; McNichol J.R.; Holland M.S.; Taisne J.P.; Lemay J. and Lorden D.J. Application Aspects of Multiterminal DC Power Transmission, *IEEE Transactions on Power Delivery*, Vol. 5, No. 4, pp. 2084-2098, Oct. 1990. DOI: 10.1109/61.103704.
- [10] Shore N. L. et al, DC Filters for Multiterminal HVDC Systems, *IEEE Transactions on Power Delivery*, Vol. 11, No. 4, Oct 1996.
- [11] Szechtman M.; Wess T. and Thio C.V.; A Benchmark Model for HVDC System Studies. *Elektra*, No 135, Apr. 1991.
- [12] Khatir M.; Zidi S.-A.; Hadjeri S.; Fellah M.-K., Dahou O.; Effect of the DC Control on Recovery from Commutation Failures in an HVDC Inverter Feeding a Weak AC Network. *Journal of Electrical Engineering*, Vol. 58, No. 4, pp. 200-206, 2007.
- [13] Vaughan R.L.; Bowles J.P.; Dalzell J.; The Control and Performance of a Series Connected Multiterminal HVDC Transmission System, *IEEE Transactions on Power Apparatus and Systems*, Vol. 94, No. 5, pp. 1868 – 1877, 1975.
- [14] ALSTOM, HVDC Connecting to the Future. 1<sup>st</sup> Ed. ALSTOM Grid, 2010.
- [15] Zou G.; Zheng J.C. and Chen X.X.; Study on Commutation Failure in an HVDC Inverter. *Int. Conf. on Power System Technology (Powercon 98)*, Vol. 1, Beijing, Aug. 1998, pp.503-506.

---

**Authors:** dr. Ricardo Leon Vasquez-Arnez, Foundation for the Technological Development of the Engineering Sciences (FDTE), E-mail: [ricardoleon00@yahoo.co.uk](mailto:ricardoleon00@yahoo.co.uk); prof. dr. Jose Antonio Jardini, Polytechnic School of the University of Sao Paulo, E-mail: [jose.jardini@gmail.com](mailto:jose.jardini@gmail.com); msc. Marcos T. Bassini, Polytechnic School of the University of Sao Paulo, E-mail: [mtbassini@gmail.com](mailto:mtbassini@gmail.com).

The correspondence address is:  
e-mail: [ricardoleon00@yahoo.co.uk](mailto:ricardoleon00@yahoo.co.uk)